International Journal of Nanomedicine

Dovepress
open access to scientific and medical research

Open Access Full Text Article

ORIGINAL RESEARCH

Involvement of TGF-β and ROS in G1 Cell Cycle Arrest Induced by Titanium Dioxide Nanoparticles Under UVA Irradiation in a 3D Spheroid Model

This article was published in the following Dove Press journal:
International Journal of Nanomedicine

Yuanyuan Ren[1]
Runqing Geng[1]
Qunwei Lu[1,2]
Xi Tan[1]
Rong Rao[1]
Hong Zhou[1]
Xiangliang Yang[1,3]
Wei Liu[1,3]

[1]College of Life Science and Technology, Huazhong University of Science and Technology, Wuhan 430074, People's Republic of China; [2]Key Laboratory of Molecular Biophysics of the Ministry of Education, College of Life Science and Technology, Center for Human Genome Research, Huazhong University of Science and Technology, Wuhan 430074, People's Republic of China; [3]National Engineering Research Center for Nanomedicine, Huazhong University of Science and Technology, Wuhan 430074, People's Republic of China

Background: As one of the most widely produced engineered nanomaterials, titanium dioxide nanoparticles (nano-TiO_2) are used in biomedicine and healthcare products, and as implant scaffolds; therefore, the toxic mechanism of nano-TiO_2 has been extensively investigated with a view to guiding application. Three-dimensional (3D) spheroid models can simplify the complex physiological environment and mimic the in vivo architecture of tissues, which is optimal for the assessment of nano-TiO_2 toxicity under ultraviolet A (UVA) irradiation.

Methods and Results: In the present study, the toxicity of nano-TiO_2 under UVA irradiation was investigated in 3D H22 spheroids cultured in fibrin gels. A significant reduction of approximately 25% in spheroid diameter was observed following treatment with 100 μg/mL nano-TiO_2 under UVA irradiation after seven days of culture. Nano-TiO_2 under UVA irradiation triggered the initiation of the TGF-β/Smad signaling pathway, increasing the expression levels of TGF-β1, Smad3, Cdkn1a, and Cdkn2b at both the mRNA and protein level, which resulted in cell cycle arrest in the G1 phase. In addition, nano-TiO_2 under UVA irradiation also triggered the production of reactive oxygen species (ROS), which were shown to be involved in cell cycle regulation and the induction of TGF-β1 expression.

Conclusion: Nano-TiO_2 under UVA irradiation induced cell cycle arrest in the G1 phase and the formation of smaller spheroids, which were associated with TGF-β/Smad signaling pathway activation and ROS generation. These results reveal the toxic mechanism of nano-TiO_2 under UVA irradiation, providing the possibility for 3D spheroid models to be used in nanotoxicology studies.

Keywords: nano-TiO_2, cell cycle arrest, TGF-β signaling pathway, reactive oxygen species, 3D spheroid culture

Correspondence: Qunwei Lu
Key Laboratory of Molecular Biophysics of the Ministry of Education, College of Life Science and Technology, Center for Human Genome Research, Huazhong University of Science and Technology, Wuhan 430074, People's Republic of China
Email luqw@hust.edu.cn

Wei Liu
College of Life Science and Technology, Huazhong University of Science and Technology, Wuhan 430074, People's Republic of China
Tel +86-27-8779-2147
Fax +86-27-8779-2234
Email wliu@hust.edu.cn

Introduction

Titanium dioxide nanoparticles (nano-TiO_2) possess excellent properties, such as a minute size, effective absorption and scattering of ultraviolet (UV) light, biocompatibility, and good osteoconduction, which have led to their increased use in cosmetics, pharmaceuticals, food products, and bone tissue engineering.[1–3] Approximately 60,000 tons of nano-TiO_2 are produced worldwide each year, and the extensive applications of nano-TiO_2 have increased the chances of human exposure over recent decades;[4,5] therefore, the potential toxic effects of nano-TiO_2 have received increasing attention.

Nano-TiO_2 with photoreactivity under UVA irradiation induce significant cell damage, lipid peroxidation, and overexpression of glycans, which leads to phototoxic reactions.[6–8] Nano-TiO_2 induce normal liver cell apoptosis by triggering the production

of a large amount of reactive oxygen species (ROS) under UVA irradiation, resulting in upregulation of the death receptor, Fas, and Bax.[1] Despite the plethora of research regarding the phototoxicity of nano-TiO_2 in vitro and in vivo, the acute toxicity of nano-TiO_2 and the underlying mechanisms remain a major concern in the assessment of nanotoxicity. In particular, little attention has been paid to changes in the cell cycle and intracellular signaling pathways caused by nano-TiO_2 under UVA irradiation. Exposure of A549 cells to 100 μg/mL anatase nano-TiO_2 for 24 h has been shown to induce ROS generation and DNA breaks, resulting in the upregulated expression of p53 and activation of cell cycle arrest in the G2/M phase.[9] Cell cycle progression is a complex and accurate process that is blocked in response to various stimuli.[10,11] The transforming growth factor-β (TGF-β) signaling pathway is activated by sub-chronic nano-TiO_2 exposure, which induces inflammation and fibrosis and also plays a pivotal role in cell proliferation, differentiation, and cell cycle regulation.[12,13] However, the effect of nano-TiO_2 under UVA irradiation on cell cycle progression and the involvement of TGF-β in its regulation have been sparsely studied. Therefore, it is imperative to systematically analyze the regulation of cell cycle progression and the underlying molecular mechanism of nano-TiO_2 under UVA irradiation.

Traditional two-dimensional (2D) cell culture models and in vivo animal models are commonly used to evaluate nanotoxicity; however, 2D models do not accurately predict in vivo toxicity and biological effects due to the simple element and lack of a microenvironment,[14,15] and animal models have a complex physiological structure that renders it difficult to elucidate molecular mechanisms. Therefore, it is necessary to develop a novel model for the rapid assessment of nanotoxicity and investigation into the toxic mechanisms of nanoparticles. Three-dimensional (3D) culture models are a promising alternative, since they provide cell−cell and cell−matrix interactions that better mimic the physiological in vivo aspects.[15–17] Human osteoblast-like spheroids treated with nano-TiO_2 have been shown to augment collagen deposition and pro-inflammatory cytokine and growth factor secretion, although no significant differences in morphology, proliferation, or cell cycle have been observed.[16] Nevertheless, the molecular mechanisms underlying the osteoblast spheroid alterations caused by nano-TiO_2 are not well understood. To date, there are few published studies regarding nano-TiO_2 under UVA irradiation in 3D spheroid models.

Prior studies by our group have established a highly effective 3D fibrin gel culture model for the generation of tumor spheroids, with which the mechanism of IFN-γ-induced immunologic dormancy was elucidated.[18,19] H22 cells are more likely to form larger multicellular tumor spheroids in 3D fibrin gels over time, which can be easily observed in subsequent experiments.[18] Moreover, liver cells play an essential role in detoxification and circulating nanoparticle clearance.[20] Different concentrations of fibrin gel solution are equivalent to different elastic forces, with 1 mg/mL having been proven to be optimal for tumor cell culture.

In the present study, 1 mg/mL fibrin gels were exploited for the first time to culture H22 tumor spheroids with a view to investigating of the effects of nano-TiO_2 under UVA irradiation. Analysis of spheroid size, cell senescence, apoptosis, and the cell cycle demonstrated that the ROS generated as a result of the action of nano-TiO_2 under UVA irradiation caused cell cycle arrest in the G1 phase via activation of the TGF-β signaling pathway, which ultimately led to cell growth inhibition and the formation of smaller tumor spheroids. Our study provides novel insight into the nanotoxicity and underlying mechanisms of nano-TiO_2 under UVA irradiation, which opens avenues for capitalizing on sophisticated 3D spheroid models in fibrin gel as an emerging tool for drug discovery and toxicity assessment.

Materials and Methods

Chemicals and Materials

Titanium dioxide nanoparticles (nano-TiO_2) were purchased from Degussa AG (Essen, Germany) at ≥ 99% purity in the form of an anatase-rutile mixture. Prior to use as a cell treatment, nano-TiO_2 were sonicated for 20 min. UVA light was provided by a UV lamp (ZF-5, 365 nm, 8 W, 0.6 mW/cm^2, Shanghai Huxi Instrument, China).

Fetal bovine serum (FBS), penicillin, streptomycin, and trypsin−EDTA were purchased from Gibco (Invitrogen, USA). RPMI 1640 medium and phosphate-buffered saline (PBS) were purchased from Hyclone (GE Healthcare). 2.7-Dichlorofluorescin diacetate (DCFH-DA), camptothecin and propidium iodide (PI) were purchased from sigma (USA). Fibrin gel and thrombin were purchased from Searun Holdings Company (Freeport, ME, USA). Dispase® II was obtained from Roche. The senescence-associated β-galactosidase (SA-β-gal) activity assay, BCA assay, annexin V-FITC/PI apoptotic detection assay, and cell cycle kits were

obtained from Beyotime. TRIzol was purchased from Invitrogen (Carlsbad, USA). The cDNA reverse transcription and real-time quantitative PCR SYBR® Green kits were obtained from TAKARA (Otsu, Japan). PVDF membrane was purchased from Millipore (MA, USA). Rabbit polyclonal anti-Smad3, anti-TGF-β1, anti-Cdkn1a, and anti-Cdkn2b antibodies were purchased from ABclonal (Boston, USA). The mouse monoclonal anti-GAPDH antibody was obtained from Univ (China). The secondary antibody, phenylmethanesulfonylfluoride (PMSF), and RIPA lysis buffer were purchased from Beyotime (China). The ECL Western blotting substrate was obtained from Thermo Fisher Scientific.

Cell Culture

H22 cells were supplied by the China Center for Type Culture Collection (Wuhan University, Wuhan, China), and were cultured in RPMI 1640 medium supplemented with 10% FBS and 1% penicillin/streptomycin at 37°C in a humidified atmosphere of 5% CO_2.

Exposure to Nano-TiO_2 Under UVA Irradiation and 3D Fibrin Gel Culture

Nano-TiO_2 was suspended in RPMI 1640 medium, sonicated for 20 min in an ultrasonic bath, and diluted to a concentration of 100 μg/mL. Following cell culture in 12-well plates for 24 h, fresh nano-TiO_2 suspensions were applied to the cells. After incubation for 4 h, the medium was replaced with PBS prior to UVA radiation at 365 nm. After irradiation for 40 min, fresh medium was added and the cells were incubated for a further 2 h.[21]

Approximately 2000 cells in 25 μL RPMI 1640 medium were mixed with 25 μL 2 mg/mL fibrin gel solution and seeded onto pre-cooled 96-well plates containing 1 μL thrombin. The solution was mixed well, and the cell culture plate was placed in a 37°C cell culture incubator for 30 min. Finally, 200 μL RPMI 1640 medium supplemented with 10% FBS and 1% penicillin/streptomycin was added.[18] The cells were trapped in the 3D fibrin gel and formed spheroids.

Cell Cycle Progression Analysis

Cell cycle progression was analyzed using PI. To harvest the 3D spheroid colonies in the soft fibrin gels, the gels were washed three times with PBS and treated with Dispase® II for 20 min at 37°C.[19] The cells were centrifuged at 1500 rpm for 5 min and fixed in cold 70% ethanol for 24 h at 4°C. The following day, the fixed cells were centrifuged at 1500 rpm for 10 min, and the pellet was resuspended in 1 mL PBS, centrifuged, and resuspended in 1 mL PI staining solution and RNase A. After incubation at 37°C for 15−30 min in the dark, the cells were analyzed by FACS (FC500, BD Biosciences, CA) to determine the cell cycle stage.[9] A concentration of 10 μg/mL camptothecin was used as a positive control.

Intracellular ROS Measurement

Intracellular ROS were measured by DCFH-DA. Cells were incubated with nano-TiO_2 under UVA irradiation and then seeded in the 3D fibrin gel. Subsequently, cells cultured in 3D fibrin gels were washed three times with PBS and incubated with medium containing 20 μL DCFH-DA at 37°C for 30 min, after which the medium was discarded and 100 μL PBS was added to each well. Qualitative analysis of ROS generation was performed using a microscope with a fluorescence attachment. The fluorescence intensity was quantitated by pixels using the NIH Image J software (Macintosh, USA).

SA-β-Gal Activity Assay

Senescence was determined by the SA-β-gal assay. Cells were treated with Dispase® II for 20 min at 37ºC, fixed for 15 min at room temperature, and stained overnight at 37ºC under CO_2 -free conditions using a β-galactosidase staining kit. SA-β-gal -positive and -negative cells were imaged by microscopy.

Apoptosis Analysis

Annexin V-FITC and PI were used to label apoptotic cells cultured in 3D fibrin gels. Briefly, cells cultured in 3D fibrin gels were rinsed with pre-warmed PBS and treated with Dispase® II for 20 min at 37°C. After centrifugation, cells were collected and incubated with 10 μg/mL PI and annexin V-FITC (pre-diluted in normal culture medium) for 15 min. The cells were detected by flow cytometry.[11] Early apoptotic cells were detected by annexin V-FITC, whereas late apoptotic and necrotic cells were identified by PI and annexin V-FITC.

Quantitative Real-Time PCR

Total RNA was extracted from H22 spheroids in 3D fibrin gels using TRIzol and transcribed to cDNA using a high-capacity cDNA reverse transcription kit.[11] Quantitative PCR was performed using SYBR® Green. The primer sequences are given in Table 1. Real-time PCR was performed using the ABI StepOnePlus™ PCR system (Applied Biosystems, MA, USA). The amplification conditions were: 1 cycle of 95°C for 3 min, followed by 40 cycles of 15 s at 95ºC and 30 s at 60°C. Target RNA levels were normalized to the *gapdh* housekeeping gene. All experiments were performed three times and the data were analyzed using the $2^{-\Delta\Delta CT}$ method.

Table 1 Sequences of the Real-Time PCR Primers

Gene	Forward Primer (5′-3′)	Reverse Primer (5′-3′)
Cdkn1a	CGAGAACGGTGGAACTTTGA	CCAGGGCTCAGGTAGACCTT
Cdkn2b	CCCTGCCACCCTTACCAGA	GCAGATACCTCGCAATGTCAC
TGF-β1	GCTAATGGTGGACCGCAA	CACTGCTTCCCGAATGTCTGA
Smad3	TCTCCCCGAATCCGATGTCC	GCTGGTTCAGCTCGTAGTAGG
Gapdh	AGGTCGGTGTGAACGGATTTG	TGTAGACCATGTAGTTGAGGTCA

Western Blotting

Cells were harvested, washed with ice-cold PBS, and resuspended in RIPA lysis buffer containing the protease inhibitor, PMSF. Lysates were sonicated, clarified by centrifugation, and quantitated using a BCA assay kit. Lysates were boiled, and 20 μg protein was separated by 12% SDS-PAGE and transferred to PVDF membrane.[22] Membranes were blocked with 5% non-fat milk and probed with the indicated primary antibodies overnight at 4°C: anti-GAPDH (0.5 μg/mL), anti-TGF-β1 (1 μg/mL), anti-Cdkn1a (1 μg/mL), anti-Cdkn2b (1 μg/mL), and anti-Smad3 (1 μg/mL). Detection was performed after incubation with HRP-conjugated secondary antibodies. The reaction was developed using Pierce ECL Western blotting substrate. Results were confirmed by at least three independent experiments. The intensity of the chemiluminescent spots was quantitatively estimated using the Quantity One software.

Statistical Analysis

Results of each experiment are expressed as the mean ± standard error of the mean from at least three individual experiments. Data were analyzed using the Student's *t*-test. For all comparisons, differences were considered statistically significant at *** $p < 0.001$ and ** $p < 0.005$.

Results

Nano-TiO_2 Under UVA Irradiation Cause Reduced Growth of Multicellular Tumor Spheroids in Fibrin Gels

The size of nano-TiO_2 used in the present study was 25 nm, the characterization of which has been described previously.[8] The crystalline composition was a mixture of rutile and anatase. From day 3 to 7, the cells were seeded in fibrin gels and imaged to evaluate 3D spheroid formation (Figure 1A). On day 7, the diameter of 3D spheroids reached approximately 63 μm. There was no difference in the size of the spheroids exposed to UVA irradiation or nano-TiO_2 alone; however, the size of the spheroids decreased dramatically to approximately 45 μm in the presence of nano-TiO_2 under UVA irradiation.

The volume of the spheroids increased as the culture time increased, up to approximately 130×10^3 μm^3 on day 7. Nano-TiO_2 under UVA irradiation led to a significantly smaller spheroid volume of approximately 55×10^3 μm^3 on day 7 (Figure 1B). The spheroids were dispersed by treatment with Dispase® II, and the cells were subsequently counted. The cell number was consistent with the data suggesting that the number of cells in the spheroids decreased in the presence of nano-TiO_2 under UVA irradiation (Figure 1C).

Nano-TiO_2 Under UVA Irradiation Do Not Impact Cell Apoptosis or Senescence in 3D Spheroids

The size of the 3D spheroids indicates the rate of proliferation of tumor cells; a slower rate of proliferation led to a smaller spheroid size. Apoptosis and senescence can cause a reduction in the proliferation rate; thus, these parameters were evaluated. Cell senescence was assessed by staining for SA-β-gal activity, and no significant differences were observed among the four groups (Figure 2A). It was demonstrated that the 3D spheroids did not undergo senescence in the 3D fibrin gel culture model. Annexin V-FITC and PI staining were used to detect apoptosis, and the results show that apoptosis was not the cause of the smaller spheroid size in the nano-TiO_2 under UVA irradiation group (Figure 2B).

Nano-TiO_2 Under UVA Irradiation Induce Cell Cycle Arrest in the G1 Phase

It was hypothesized that growth arrest of tumor cells in fibrin gels resulting from treatment with nano-TiO_2 under UVA irradiation may be a crucial determinant of spheroid size; thus, PI staining was used to examine cell cycle progression. There were no significant differences in the cell cycle following exposure to nano-TiO_2 or UVA irradiation alone as compared with the control group (Figure 3). Nevertheless, after seven days of culture, a significant change in the cell cycle was observed in the nano-TiO_2 under UVA irradiation group, with the proportion of cells in the G1/S phase increasing by 1.8-fold as compared with that in the control group (Figure 3B). These data suggest that nano-TiO_2 under UVA irradiation induced cell cycle arrest in the G1 phase.

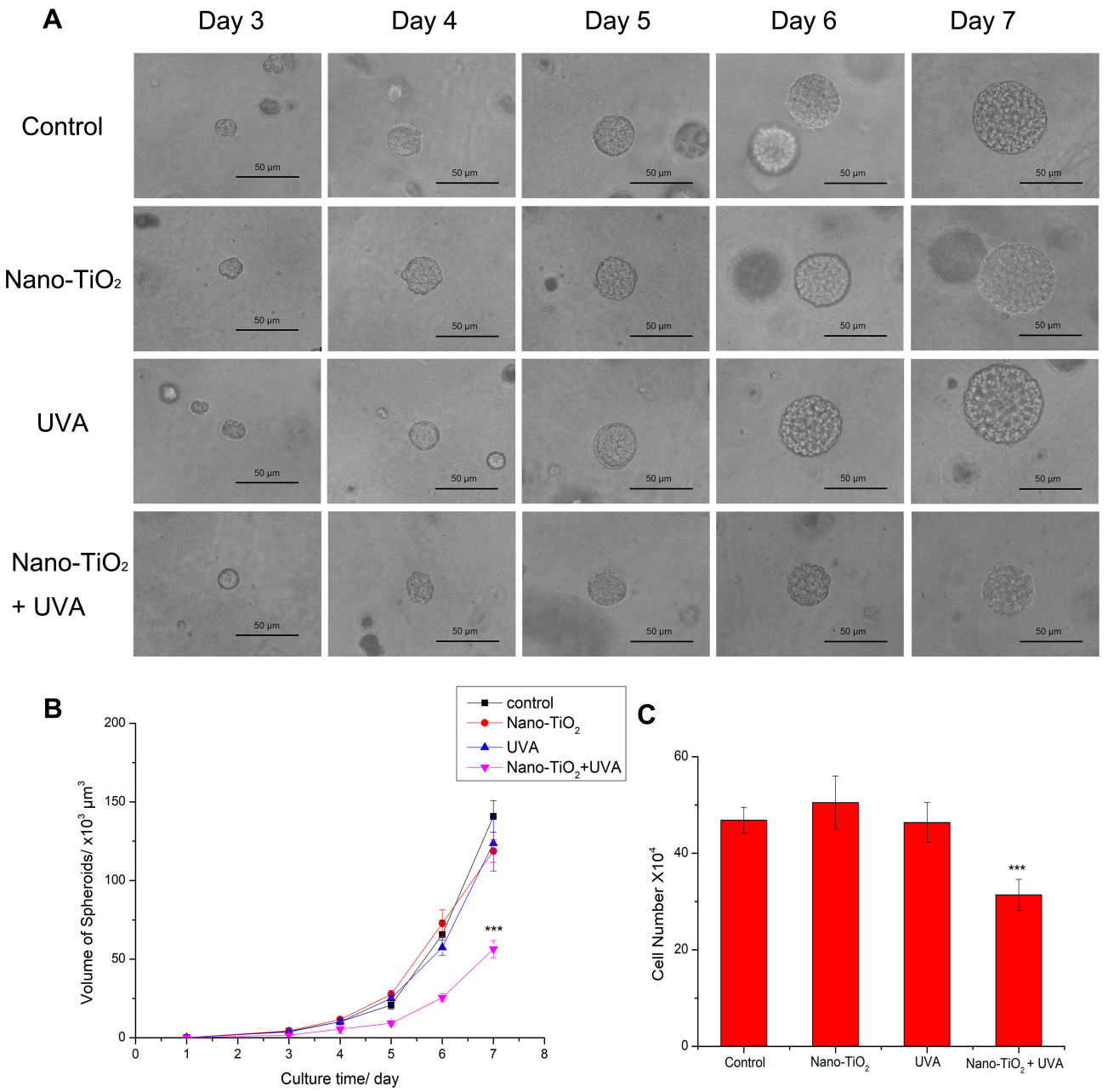

Figure 1 3D spheroid formation in fibrin gels following nano-TiO_2 and UVA irradiation treatment. (**A**) H22 cells were treated with 100 μg/mL nano-TiO_2, UVA irradiation, or nano-TiO_2 under UVA irradiation, and seeded into fibrin gels. Spheroid growth was recorded from day 3 to 7. (**B**) The volume of the spheroids was calculated. (**C**) The number of cells in each well was counted after 7 days of culture.

Notes: Data are reported as the mean ± standard error of the mean (n = 6), ***$p < 0.001$, as compared with the control group. Scale bar indicates 50 μm.

Abbreviation: UVA, ultraviolet A.

Nano-TiO_2 Under UVA Irradiation Promote Cell Cycle-Related Protein Expression

The cell cycle is closely related to cyclin-dependent kinases (CDK), which can be activated by cyclins or inhibited by CDK inhibitors.[10] Cdkn1a and Cdkn2b, are CDK inhibitor proteins involved in the transition from the G1 to the S phase of the cell cycle.[23,24] Smad transcription factors participate in the regulation of the expression of Cdkn1a and Cdkn2b.[25,26] The mRNA levels of the specific cell cycle-related genes were examined to investigate the molecular mechanisms underlying cell cycle arrest induced by nano-TiO_2 under UVA irradiation in the 3D spheroid model. The expression levels of *Cdkn1a, Cdkn2b*, and *Smad3* were significantly upregulated following treatment with nano-TiO_2 under UVA irradiation. In particular, the mRNA expression levels of *Cdkn1a* and *Cdkn2b* were upregulated by 10-fold (Figure 4A and B). In addition, the mRNA

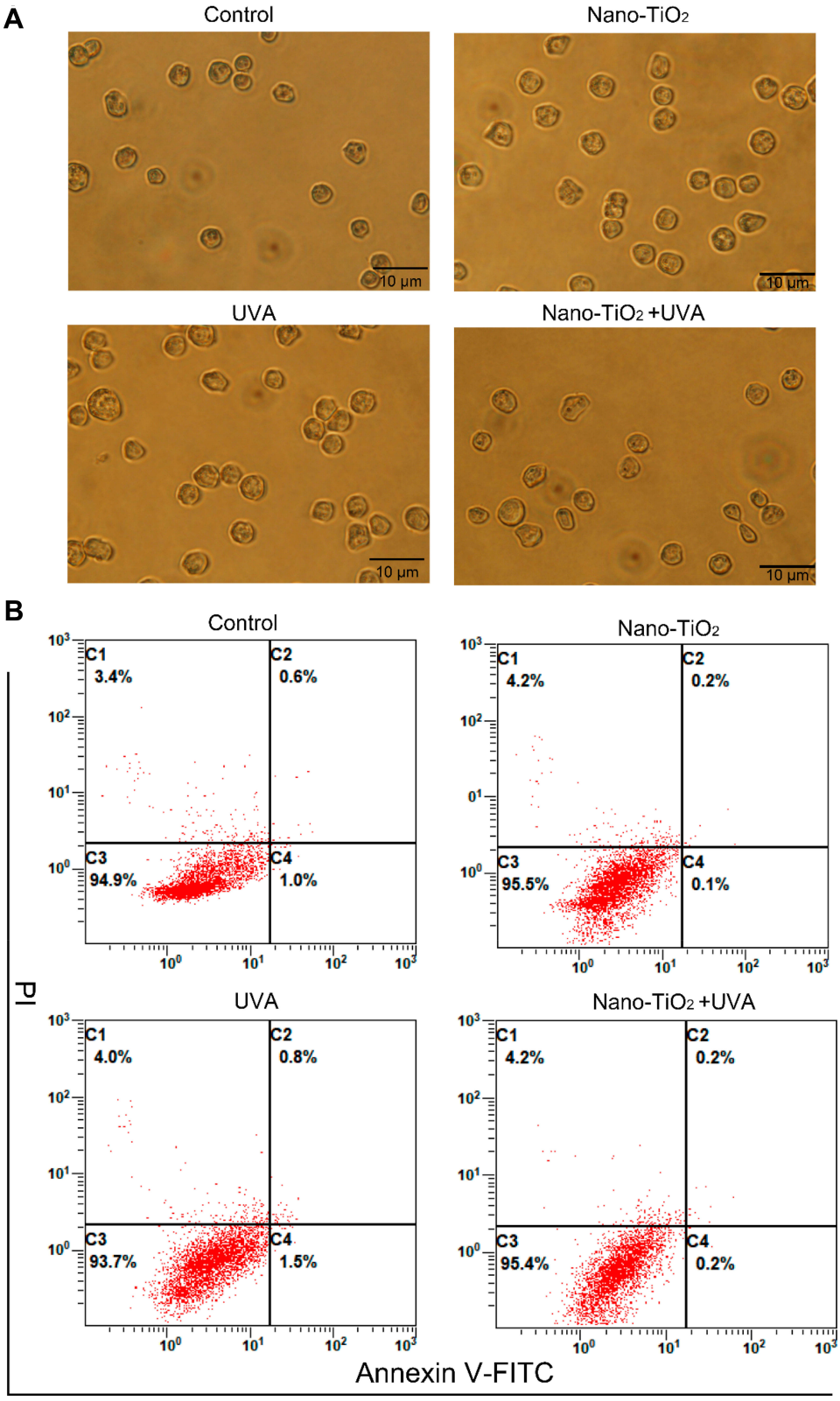

Figure 2 Cell senescence and apoptosis as shown by the SA-β-gal and annexin V-FITC/PI assays. H22 cells were treated with 100 μg/mL nano-TiO_2, UVA irradiation, or nano-TiO_2 under UVA irradiation, and seeded into fibrin gels. (**A**) SA-β-gal staining was conducted to assess cell senescence. (**B**) Annexin V-FITC/PI staining was conducted to assess cell apoptosis.

Notes: Scale bar indicates 10 μm. The four quadrants represent normal (C3), early apoptotic (C4), late apoptotic or necrotic (C2), and mechanically damaged cells (C1), respectively.

Abbreviations: UVA, ultraviolet A; SA-β, senescence-associated β-galactosidase; PI, propidium iodide.

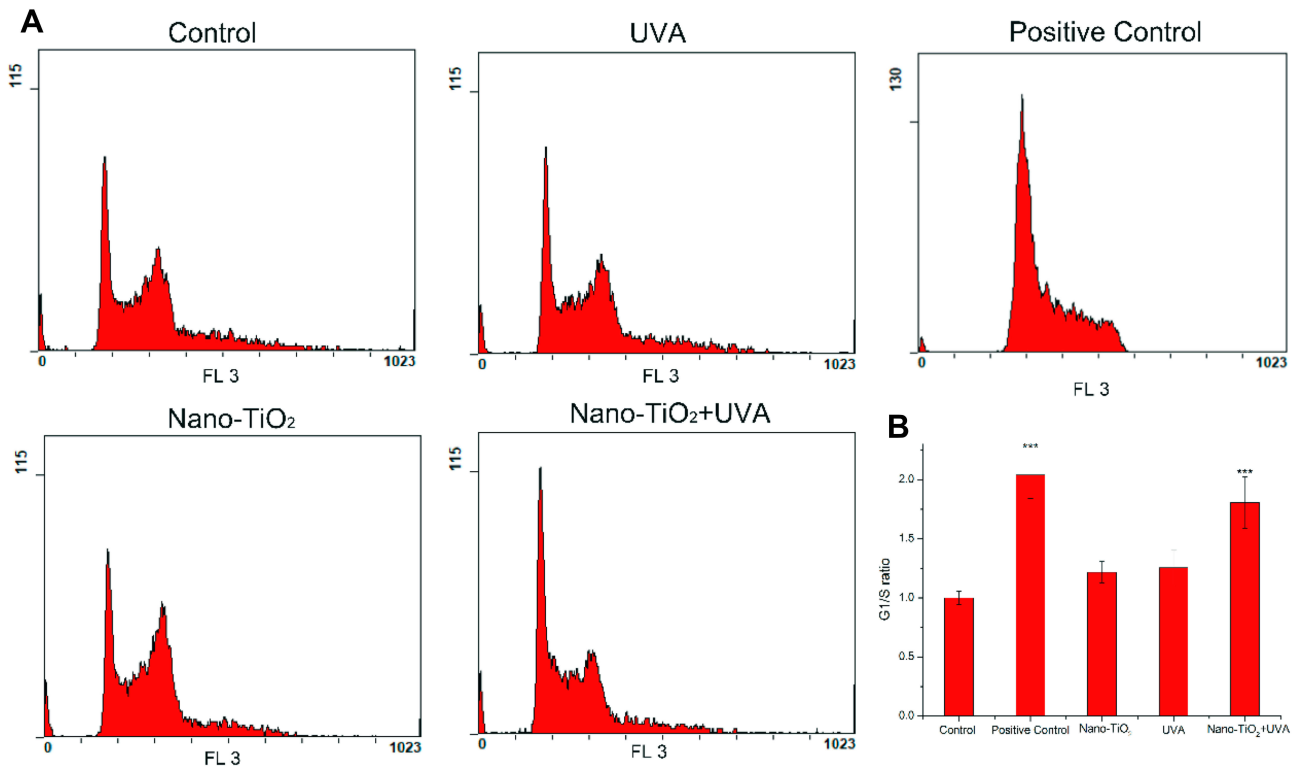

Figure 3 Cell cycle analysis in 3D spheroids after 7 days of culture. (**A**) Flow cytometry analysis of the cell cycle. PI, a DNA-specific intercalating dye, was used to stain the cells; 10 μg/mL camptothecin was used as a positive control. (**B**) Quantitative analysis of cells in the G1/S phase based on flow cytometry data. The G1/S ratio of the control group was set to 1.

Notes: Data are reported as the mean ± standard error of the mean (n = 3), ***$p < 0.001$, as compared with the control group.

Abbreviation: UVA, ultraviolet A.

expression level of *Smad3* was increased by 7-fold (Figure 4C). The protein expression levels of Cdkn1a, Cdkn2b, and Smad3 were measured by Western blotting (Figure 4D and E), which revealed significant increases in the expression of these proteins in spheroids treated with nano-TiO_2 under UVA as compared with the control group. The protein expression levels of Cdkn2b and Smad3 were increased slightly following treatment with nano-TiO_2 or UVA irradiation alone. These data indicate that nano-TiO_2 under UVA repressed the G1/S phase transition, in part, by upregulating the levels of Cdkn1a and Cdkn2b.

Nano-TiO_2 Under UVA Treatment Promote the Expression of TGF-β1

Cdkn2b is an important mediator of the antiproliferative effects of TGF-β, and Smad transcription factors are involved in the TGF-β signaling pathway. To verify whether the TGF-β signaling pathway was activated in the nano-TiO_2 under UVA irradiation group, the mRNA and protein expression levels of TGF-β1 were detected. *TGF-β1* mRNA was increased by 2.5-fold following treatment with nano-TiO_2 under UVA irradiation (Figure 5A), and TGF-β1 protein expression was increased by approximately 75% (Figure 5B). Thus, further investigation was performed to determine whether TGF-β1 induced cell cycle arrest in the G1 phase. Cells were treated with 20 ng/mL TGF-β1 and subjected to flow cytometry analysis. The results show that the total proportion of cells in the G1/S phase increased by 1.5-fold as compared with that of control cells (Figure 5C). The 3D spheroids of cells treated with 20 ng/mL TGF-β1 were smaller than the spheroids of untreated cells (Figure 5D and E). These data suggest that G1/S phase arrest induced by nano-TiO_2 under UVA irradiation was mediated by the TGF-β signaling pathway.

Nano-TiO_2 Under UVA Irradiation Inhibit Cell Cycle by Inducing the Generation of Intracellular ROS

Following confirmation that nano-TiO_2 under UVA irradiation could induce the generation of ROS within cells, ROS generation in 3D spheroids of cells treated with nano-TiO_2 under UVA was analyzed to investigate its involvement in the induction of G1/S phase arrest. The fluorescence microscopy image

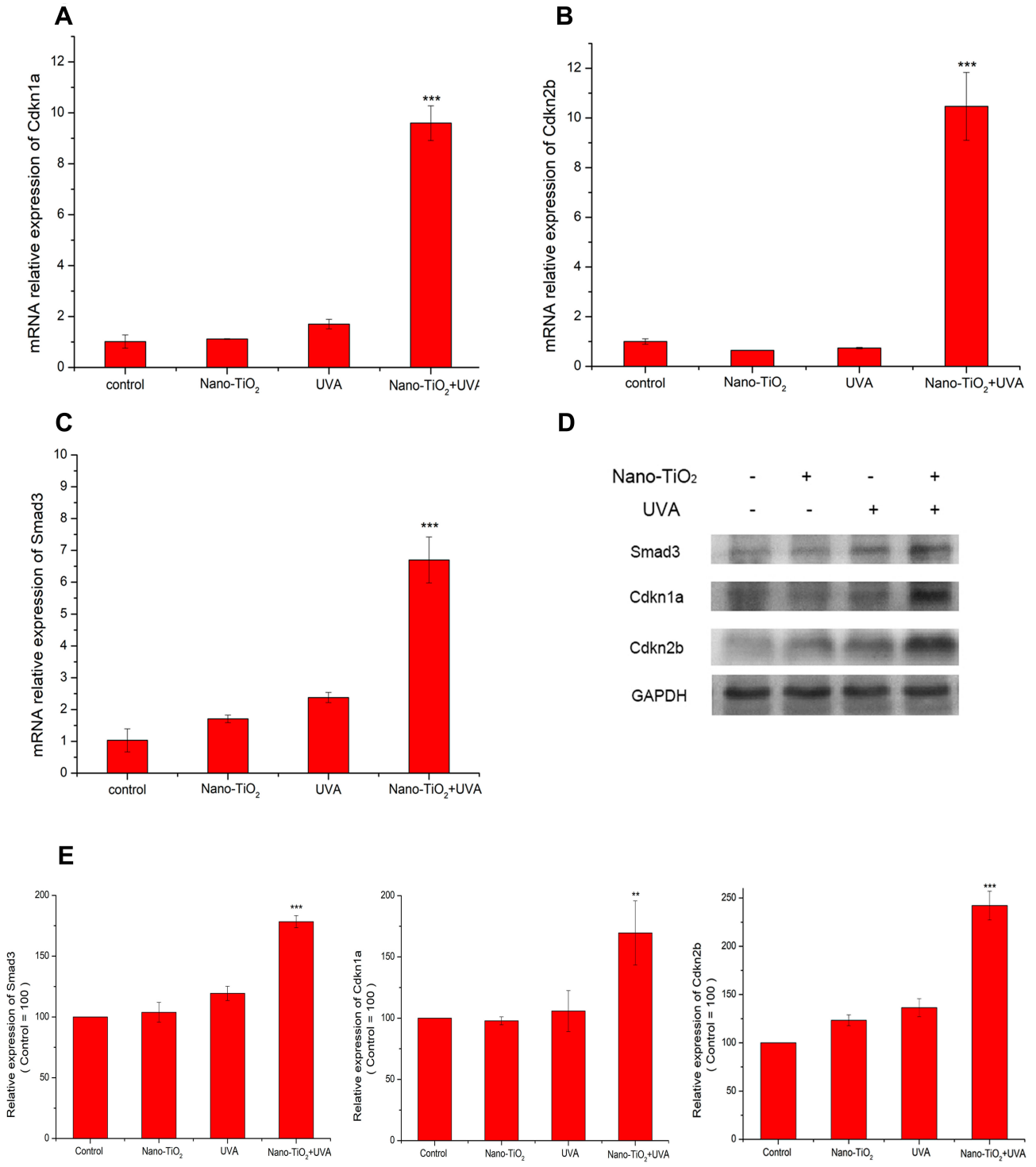

Figure 4 The expression of specific marker genes, Cdnk1a, Cdkn2b, and Smad3, in cell cycle arrest. The mRNA expression levels of *Cdnk1a* (**A**), *Cdkn2b* (**B**), and *Smad3* (**C**) were measured by real-time PCR. (**D**) The protein expression levels of Cdnk1a, Cdkn2b, and Smad3 were measured by Western blotting. (**E**) Statistics of the relative band intensities in (**D**). GAPDH served as a loading control, and the control group was set to 100.

Notes: Data are reported as the mean ± standard error of the mean (n = 3), ***$p < 0.001$, **$p < 0.005$, as compared with the control group.

Abbreviation: UVA, ultraviolet A.

demonstrates that the level of intracellular ROS generated in the spheroids changed following different treatments (Figure 6A). The smaller 3D spheroids, which were formed following exposure to nano-TiO_2 under UVA irradiation, exhibited a greater level of ROS as compared with the other spheroids. H_2O_2 was used as a positive control to stimulate the

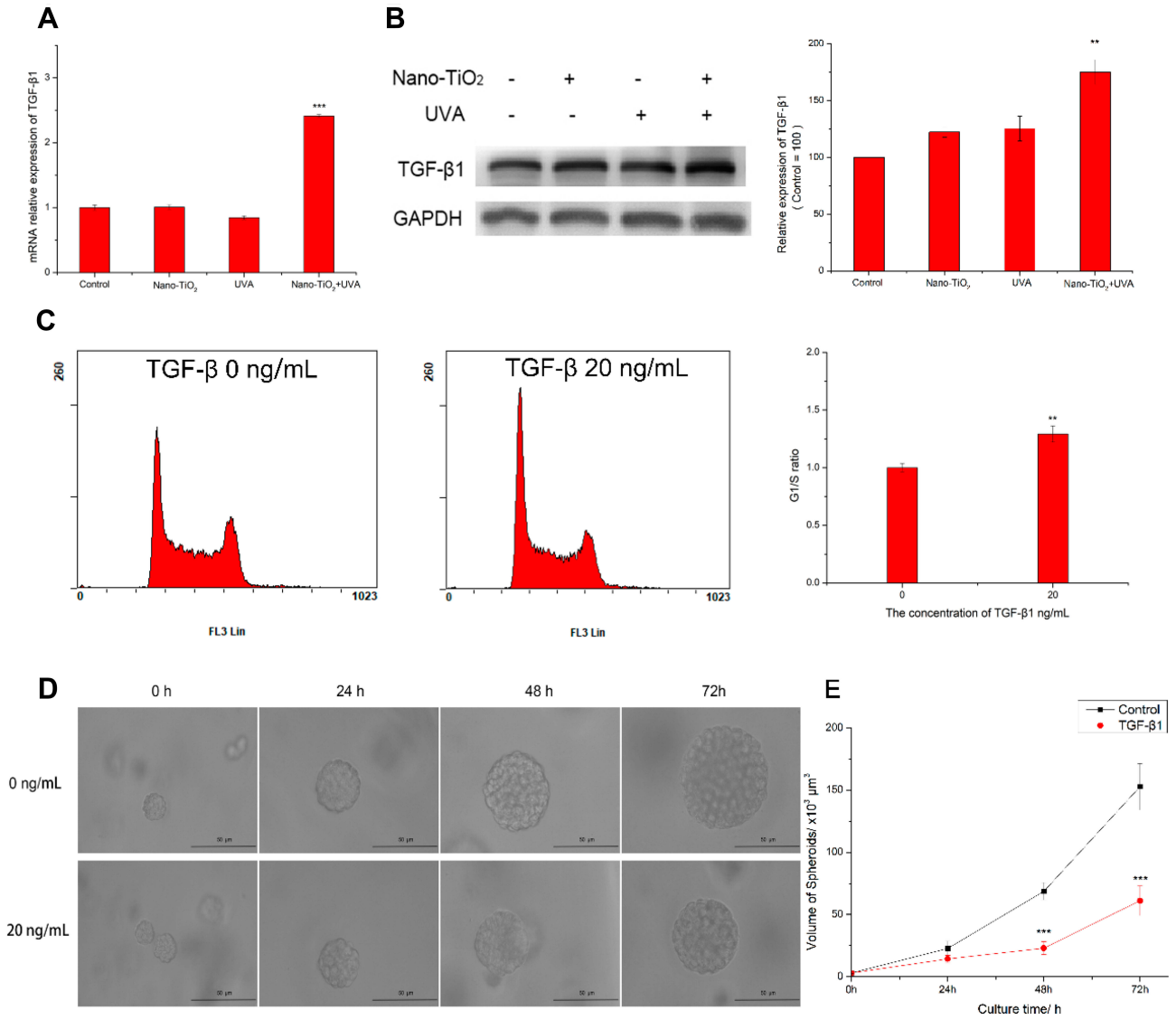

Figure 5 Cell cycle arrest in 3D spheroids of cells treated with nano-TiO_2 under UVA irradiation is regulated by TGF-β. (**A**) The mRNA expression level of *TGF-β1* in the spheroids were measured by real-time PCR. (**B**) The protein expression level of TGF-β1 in the spheroids was measured by Western blotting. GAPDH served as a loading control, and the control group was set to 100. (**C**) Cell cycle alterations following treatment of cells with TGF-β1. The G1/S ratio of the control group was set to 1. (**D**) The effects of TGF-β1 on spheroid size in 3D fibrin gels. (**E**) The volume of the spheroids was calculated.

Notes: Data are reported as the mean ± standard error of the mean (n = 3), ***$p < 0.001$, **$p < 0.005$, as compared with the control group. Scale bar indicates 50 μm.

Abbreviations: UVA, ultraviolet A; TGF-β1, transforming growth factor-β1.

production of intracellular ROS. H22 cells treated with 100 μM H_2O_2 displayed growth arrest in the G1 phase of the cell cycle, indicating that nano-TiO_2 under UVA irradiation induced the generation of ROS, which slowed proliferation by arresting the cells in the G1 phase (Figure 6B). Moreover, treatment with vitamin C, an antioxidant, eliminated the ROS production induced by nano-TiO_2 under UVA irradiation, which decreased the proportion of cells in the G1 phase (Figure S1). To investigate the underlying mechanism of cell cycle regulation by ROS, the expression of TGF-β1 was measured after exposure to H_2O_2 for 48 h (Figure 6C). Western blotting shows that the protein expression level of TGF-β1 was increased significantly in the treated group as compared with the controls. Moreover, the protein expression levels of Smad3, Cdkn1a, and Cdkn2b were increased (Figure S2). Taken together, these data indicate that ROS generation induced by nano-TiO_2 under UVA irradiation arrested the cell cycle in the G1 phase via activation of the TGF-β signaling pathway.

Discussion

Nano-TiO_2, as one of the top five nanoparticles in annual production, is widely applied in industries ranging from healthcare to drug delivery.[3,27] The properties of nano-TiO_2, such as the minute size, photocatalytic activity, and

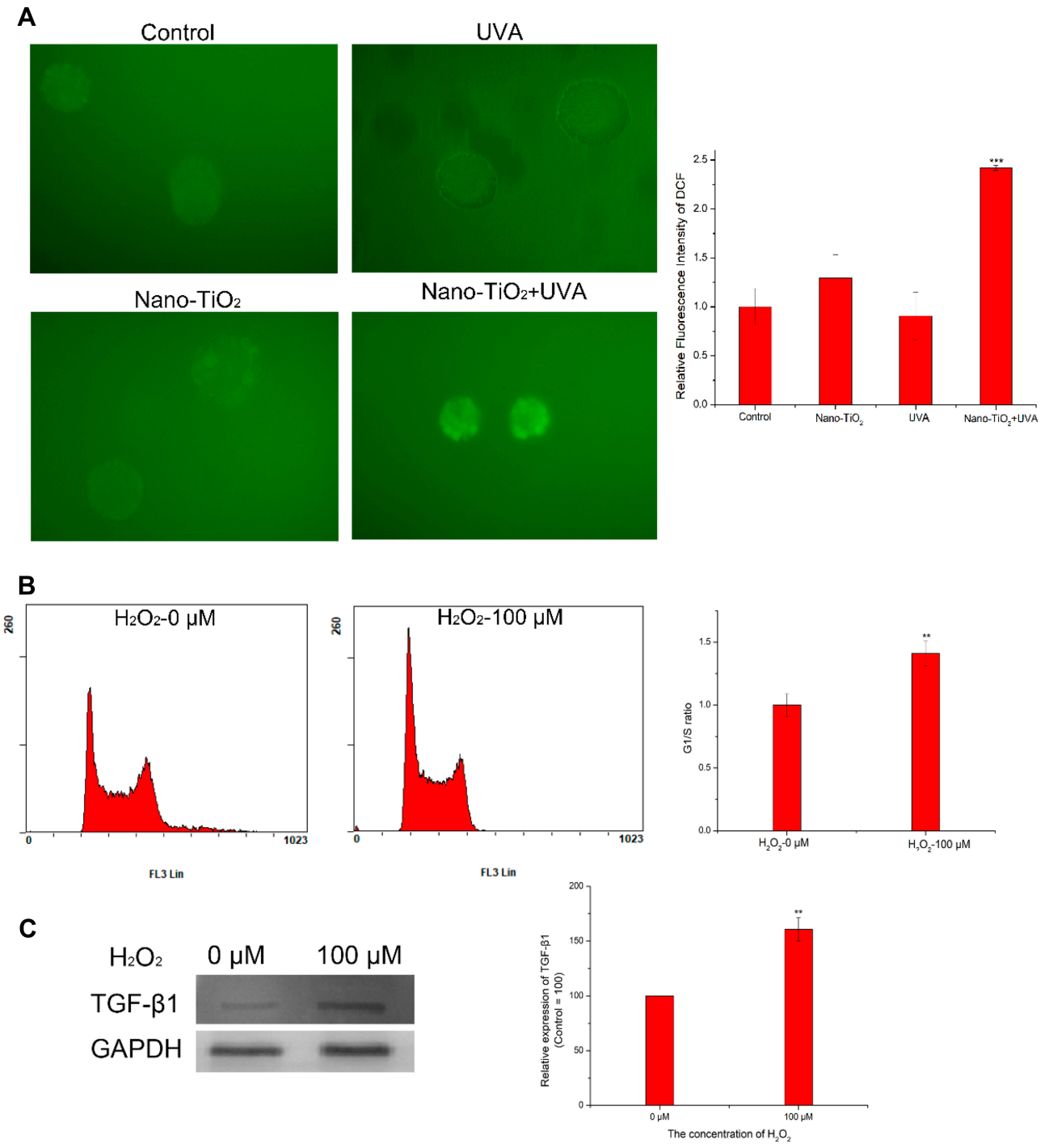

Figure 6 The generation of ROS in 3D spheroids and the effects on the cell cycle. (**A**) DCFH-DA was used to detect ROS by fluorescence microscopy. (**B**) Cell cycle of H22 cells treated with 100 μM H_2O_2 for 48 h. (**C**) The protein expression level of TGF-β1 after H_2O_2 treatment. GAPDH served as a loading control, and the control group was set to 100.

Notes: Data are reported as the mean ± standard error of the mean (n = 3), ***$p < 0.001$, **$p < 0.005$, as compared with the control group.

Abbreviations: UVA, ultraviolet A; TGF-β1, transforming growth factor-β1.

high biological reactivity, have raised concerns regarding toxicity. UVA, from 315 nm to 400 nm, constitutes the major UV irradiation in sunlight, which penetrates the epidermis and basal germinative layers, and is clearly related to human skin cancer.[28,29] Moreover, the photocatalytic activity of nano-TiO_2 under UVA irradiation from sunlight has been shown to cause severe damage,[7,30] such as the induction of HaCaT cell apoptosis,[31] inhibition of green algal growth,[32] bacterial death.[33] However, research regarding nano-TiO_2 under

UVA irradiation relies on 2D cell and in vivo animal models, which are not ideal.

In our previous study, a highly effective 3D spheroid culture system was established by culturing cancer cells in fibrin gels.[18] Fibrin gels form a 3D matrix that is utilized for injury repair in vivo,[34] the delivery of cytokines,[35] and as a support for cell growth. Fibrin gel culture systems for the assessment of nanoparticle toxicity remain unexplored; therefore, in the present study, fibrin gels were used to establish a 3D spheroid model for the assessment of nano-TiO_2 toxicity under UVA irradiation. The same number of cells following different treatments were seeded into fibrin gels and allowed to form 3D spheroids. After seven days of culture, the round morphology of the spheroids was obvious and the diameter of the spheroids reached approximately 63 μm; however, following treatment with nano-TiO_2 under UVA irradiation, the diameter only reached approximately 45 μm. The differences in the volume of the 3D spheroids are shown in Figure 1. There was no significant difference in the size of the spheroids treated with nano-TiO_2 or UVA irradiation alone as compared with the control group. In accordance with our results, no significant differences in spheroid proliferation was seen in osteoblast spheroids cultured in agarose following exposure to nano-TiO_2.[16] The formation of smaller colonies following treatment with nano-TiO_2 under UVA irradiation suggested a lower proliferation rate as compared with the control, nano-TiO_2, and UVA groups; therefore, the number of cells in the 3D spheroids was counted, verifying that larger colonies contained more cells due to a higher proliferation rate.

Subsequently, the mechanism by which nano-TiO_2 under UVA irradiation influenced 3D spheroid size was investigated. Cell senescence and apoptosis can inhibit cell growth and lead to a reduced number of cells; however, the spheroids were shown to not undergo senescence or apoptosis, as assessed by staining for SA-β-gal activity and annexin V/PI. These data suggest that senescence and apoptosis were not key factors in the formation of smaller spheroids following treatment with nano-TiO_2 under UVA irradiation (Figure 2). Further, cell cycle analysis revealed that the proportion of cells in the G1/S phase increased significantly following treatment with nano-TiO_2 under UVA irradiation as compared with that in the control group (Figure 3). These data suggest that the reduction in cell proliferation during spheroid formation was likely caused by cell cycle arrest.

Since the cell cycle is closely associated with cell proliferation and cytotoxicity, clarifying the mechanism by which nano-TiO_2 under UVA irradiation regulate the cell cycle is of great importance.[36] Cdkn1a and cdkn2b are key cell cycle regulators in G1/S transition, which inhibit the activity of CDK2 or CDK4, respectively, to regulate cell cycle progression from the G1 phase;[24,26] therefore, changes in the expression levels of Cdkn1a and Cdkn2b were evaluated in the present study. At the mRNA level, upregulation of *Cdkn1a* and *Cdkn2b* in spheroids of cells treated with nano-TiO_2 under UVA irradiation is in accordance with observations regarding the cell cycle (Figure 4). Western blotting further confirmed that the protein expression levels of Cdkn1a and Cdn2b were increased in cells arrested in the G1 phase following treatment with nano-TiO_2 under UVA irradiation.

It has been previously reported that Cdkn2b is a pivotal mediator in the TGF-β/Smad signaling pathway during the regulation of cell cycle progression;[10] therefore, it is reasonable to hypothesize that TGF-β/Smad signaling may be involved in G1 arrest induced by nano-TiO_2 under UVA irradiation. Smad3, in cooperation with additional cofactors, has been shown to induce upregulated expression of Cdkn1a and Cdkn2b, causing cell cycle arrest in G1.[25,37] Here, it is shown that the expression levels of TGF-β1 and its downstream effector, Smad3, were increased significantly following treatment with nano-TiO_2 under UVA irradiation, while no significant changes were observed in the nano-TiO_2 or UVA groups (Figures 4 and 5). These data are consistent with a previous report demonstrating that nanoparticle exposure markedly increases TGF-β1 in both in vivo and in vitro experiments.[38] An increased proportion of cells in G1/S was observed following treatment with 20 μg/mL TGF-β1 in the present study. Similar observations that TGF-β1 causes cell growth arrest in the G1 phase by means of regulating the expression levels of Smad3, p-Smad3, Cdkn1a, Cdkn2b, P16, and P18 have been previously reported.[39,40] The mechanism underlying the formation of smaller 3D spheroids following treatment with nano-TiO_2 under UVA irradiation is likely related to the activation of the TGF-β/Smad signaling pathway, leading to an increase in the expression levels of Cdkn1a and Cdkn2b and subsequent arrest of the cell cycle in the G1 phase, which inhibits cell growth in 3D fibrin gel model.

The involvement of ROS in cell cycle arrest has been previously reported. The oxygen-rich environment created by ROS generation results in G1 cell cycle arrest, and glutathione (a ROS inhibitor) attenuates this effect.[13,41] In the present study, it was observed that nano-TiO_2 under UVA irradiation enhanced the levels of ROS (Figure 6A). To further confirm whether ROS was related to cell cycle arrest in the G1 phase, H_2O_2 was employed as a positive control. A significant increase in the percentage

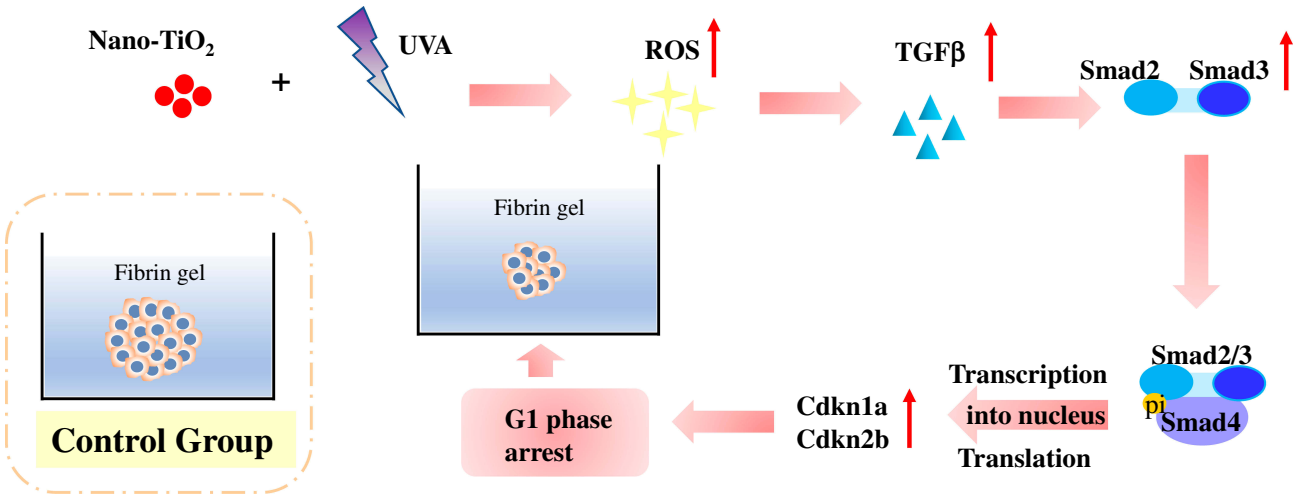

Figure 7 Possible mechanism involved in cell cycle arrest in 3D spheroids induced by nano-TiO_2 under UVA irradiation.
Abbreviations: UVA, ultraviolet A; ROS, reactive oxygen species; TGF-β1, transforming growth factor-β1.

of cells in the G1/S phase was found following treatment with 100 μM H_2O_2 as compared with that in the control group. Moreover, vitamin C alleviated the cell cycle arrest caused by treatment with nano-TiO_2 under UVA irradiation (Figure S1). These results indicate that nano-TiO_2 under UVA irradiation induced H22 cell cycle arrest in the G1 phase, resulting in the formation of smaller spheroids via the induction of ROS generation.

TGF-β/Smad signaling is ROS-sensitive and can be blocked by the ROS-inhibiting enzyme, superoxide dismutase (SOD);[42,43] thus, to identify whether ROS production caused TGF-β/Smad signaling activation, the expression levels of TGFβ-1, Smad2, Cdkn1a, and Cdkn2b were evaluated. It was shown that the expression levels of these proteins were increased significantly following H_2O_2 treatment as compared with those in the control group (Figure 6 and S2). Treatment with nano-TiO_2 under UVA irradiation likely induced cell cycle arrest due to the presence of increased levels of ROS, which in turn activated TGF-β/Smad signaling. After a long culture period in 3D fibrin gels, there was a visible difference in spheroid size (Figure 7).

In summary, the present study shows that nano-TiO_2 under UVA irradiation inhibited cell cycle progression from the G1 phase by stimulating the generation of ROS, thus activating the TGFβ/Smad signaling pathway and upregulating the expression of Cdkn1a and Cdkn2b in a 3D spheroid model. Intriguingly, from a different perspective, a dual effect of nano-TiO_2 under UVA irradiation was analyzed based on the results in 3D spheroids composed of H22 tumor cells. On one hand, the TGF-β/Smad signaling pathway was activated by treatment with nano-TiO_2 under UVA irradiation, causing growth inhibition as a side effect; on the other hand, nano-TiO_2 could be a potential candidate for a controlled anti-tumor agent with a UVA switch.

Conclusions

In the present study, the effect of nano-TiO_2 under UVA irradiation in a 3D fibrin gel spheroid model was described for the first time, in addition to its application in the assessment of nanotoxicity. Spheroid size, senescence, apoptosis, and signaling pathways were explored in the 3D model. After seven days of culture, spheroids of cells treated with nano-TiO_2 under UVA irradiation were smaller than those in the control group, which was attributed to cell cycle arrest in the G1 phase instead of apoptosis or senescence. The generation of ROS induced by nano-TiO_2 under UVA irradiation in 3D spheroids contributed to cell cycle arrest during spheroid formation. With respect to the underlying mechanism, the TGF-β/Smad signaling pathway was involved in the regulation of cell cycle progression by stimulating the expression of Cdkn1a and Cdkn2b, which was mediated by ROS generation. Together, these effects may explain the toxicity of nano-TiO_2 under UVA irradiation. The present study attempted to apply 3D fibrin gel culture techniques to toxicity evaluation with a view to facilitating a more comprehensive understanding of the toxicity of nanoparticles.

Acknowledgments

The authors acknowledge support by the Natural Science Foundation of China (NSFC, 31470968). The authors

thank the Analytical and Testing Center of the College of Life Science and Technology in Huazhong University of Science and Technology for their help with fluorescence microscopy and flow cytometry.

Disclosure

The authors report no conflicts of interest in this work.

References

1. Yoo K-C, Yoon C-H, Kwon D, et al. Titanium dioxide induces apoptotic cell death through reactive oxygen species-mediated Fas upregulation and Bax activation. *Int J Nanomedicine*. 2012;7:1203–1214. doi:10.2147/IJN.S28647
2. Ahn T-K, Lee DH, Kim T-S, et al. Modification of titanium implant and titanium dioxide for bone tissue engineering. In: Chun HJ, Park K, Kim C-H, Khang G, editors. *Novel Biomaterials for Regenerative Medicine*. Singapore: Springer Singapore; 2018:355–368.
3. Niska K, Pyszka K, Tukaj C, Wozniak M, Radomski MW, Inkielewicz-Stepniak I. Titanium dioxide nanoparticles enhance production of superoxide anion and alter the antioxidant system in human osteoblast cells. *Int J Nanomedicine*. 2015;10:1095–1107. doi:10.2147/IJN.S73557
4. Xu Y, Wei M-T, Ou-Yang HD, et al. Exposure to TiO2 nanoparticles increases Staphylococcus aureus infection of HeLa cells. *J Nanobiotechnology*. 2016;14(1):34. doi:10.1186/s12951-016-0184-y
5. Gomes SIL, Roca CP, von der Kammer F, Scott-Fordsmand JJ, Amorim MJB. Mechanisms of (photo)toxicity of TiO_2 nanomaterials (NM103, NM104, NM105): using high-throughput gene expression in Enchytraeus crypticus. *Nanoscale*. 2018;10(46):21960–21970. doi:10.1039/C8NR03251C
6. Sanders K, Degn LL, Mundy WR, et al. In vitro phototoxicity and hazard identification of nano-scale titanium dioxide. *Toxicol Appl Pharmacol*. 2012;258(2):226–236. doi:10.1016/j.taap.2011.10.023
7. Yin JJ, Liu J, Ehrenshaft M, et al. Phototoxicity of nano titanium dioxides in HaCaT keratinocytes–generation of reactive oxygen species and cell damage. *Toxicol Appl Pharmacol*. 2012;263(1):81–88. doi:10.1016/j.taap.2012.06.001
8. Ren Y, Liu X, Geng R, et al. Increased level of α2,6-sialylated glycans on HaCaT cells induced by titanium dioxide nanoparticles under UV radiation. *Nanomaterials*. 2018;8(4):253. doi:10.3390/nano8040253
9. Kansara K, Patel P, Shah D, et al. TiO2 nanoparticles induce DNA double strand breaks and cell cycle arrest in human alveolar cells. *Environ Mol Mutagen*. 2015;56(2):204–217. doi:10.1002/em.v56.2
10. Lavarone A, Massagué J. Repression of the CDK activator Cdc25A and cell-cycle arrest by cytokine TGF-β in cells lacking the CDK inhibitor p15. *Nature*. 1997;387(6631):417–422. doi:10.1038/387417a0
11. Gao F, Ma N, Zhou H, et al. Zinc oxide nanoparticles-induced epigenetic change and G2/M arrest are associated with apoptosis in human epidermal keratinocytes. *Int J Nanomedicine*. 2016;11:3859–3874. doi:10.2147/IJN.S107021
12. Hong F, Wu N, Ge Y, et al. Nanosized titanium dioxide resulted in the activation of TGF-β/Smads/p38MAPK pathway in renal inflammation and fibration of mice. *J Biomed Mater Res Part A*. 2016;104(6):1452–1461. doi:10.1002/jbm.a.v104.6
13. Zhao S-J, Wang X-J, Wu Q-J, et al. Induction of G1 cell cycle arrest in human glioma cells by salinomycin through triggering ROS-mediated DNA damage in vitro and in vivo. *Neurochem Res*. 2017;42(4):997–1005. doi:10.1007/s11064-016-2132-5
14. Muoth C, Wichser A, Monopoli M, et al. A 3D co-culture microtissue model of the human placenta for nanotoxicity assessment. *Nanoscale*. 2016;8(39):17322–17332. doi:10.1039/C6NR06749B
15. Štampar M, Tomc J, Filipič M, Žegura B. Development of in vitro 3D cell model from hepatocellular carcinoma (HepG2) cell line and its application for genotoxicity testing. *Arch Toxicol*. 2019;93(11):3321–3333. doi:10.1007/s00204-019-02576-6
16. Souza W, Piperni SG, Laviola P, et al. The two faces of titanium dioxide nanoparticles bio-camouflage in 3D bone spheroids. *Sci Rep*. 2019;9(1):9309. doi:10.1038/s41598-019-45797-6
17. Teichmann M, Kretschy N, Kopf S, et al. Inhibition of tumour spheroid-induced prometastatic intravasation gates in the lymph endothelial cell barrier by carbamazepine: drug testing in a 3D model. *Arch Toxicol*. 2014;88(3):691–699. doi:10.1007/s00204-013-1183-5
18. Liu J, Tan Y, Zhang H, et al. Soft fibrin gels promote selection and growth of tumorigenic cells. *Nat Mater*. 2012;11(8):734. doi:10.1038/nmat3361
19. Liu Y, Liang X, Yin X, et al. Blockade of IDO-kynurenine-AhR metabolic circuitry abrogates IFN-γ-induced immunologic dormancy of tumor-repopulating cells. *Nat Commun*. 2017;8(1):15207. doi:10.1038/ncomms15207
20. Choi K, Riviere JE, Monteiro-Riviere NA. Protein corona modulation of hepatocyte uptake and molecular mechanisms of gold nanoparticle toxicity. *Nanotoxicology*. 2017;11(1):64–75. doi:10.1080/17435390.2016.1264638
21. Xue C, Wu J, Lan F, et al. Nano titanium dioxide induces the generation of ROS and potential damage in HaCaT cells under UVA irradiation. *J Nanosci Nanotechnol*. 2010;10(12):8500. doi:10.1166/jnn.2010.2682
22. Dong H-W, Wang K, Chang -X-X, et al. Beta-ionone-inhibited proliferation of breast cancer cells by inhibited COX-2 activity. *Arch Toxicol*. 2019;93(10):2993–3003. doi:10.1007/s00204-019-02550-2
23. Fuxe J, Akusjarvi G, Goike HM, Roos G, Collins VP, Pettersson RF. Adenovirus-mediated overexpression of p15INK4B inhibits human glioma cell growth, induces replicative senescence, and inhibits telomerase activity similarly to p16INK4A. *Cell Growth Differ*. 2000;11(7):373–384.
24. Mandal M, Bandyopadhyay D, Goepfert TM, Kumar R. Interferon-induces expression of cyclin-dependent kinase-inhibitors p21WAF1 and p27Kip1 that prevent activation of cyclin-dependent kinase by CDK-activating kinase (CAK). *Oncogene*. 1998;16(2):217–225. doi:10.1038/sj.onc.1201529
25. Derynck R, Zhang Y, Feng X-H. Transcriptional activators of TGF-β responses: smads. *Cell*. 1998;95(6):737–740. doi:10.1016/S0092-8674(00)81696-7
26. Feng X-H, Liang -Y-Y, Liang M, Zhai W, Lin X. Direct interaction of c-Myc with Smad2 and Smad3 to Inhibit TGF-β-mediated induction of the CDK inhibitor p15Ink4B. *Mol Cell*. 2002;9(1):133–143. doi:10.1016/S1097-2765(01)00430-0
27. Wang M, Yang Q, Long J, et al. A comparative study of toxicity of TiO_2, ZnO, and Ag nanoparticles to human aortic smooth-muscle cells. *Int J Nanomedicine*. 2018;13:8037–8049. doi:10.2147/IJN.S188175
28. Halliday GM, Byrne SN, Damian DL. Ultraviolet A radiation: its role in immunosuppression and carcinogenesis. *Semin Cutaneous Med Surg*. 2011;30(4):214–221. doi:10.1016/j.sder.2011.08.002
29. He -Y-Y, Council SE, Feng L, Chignell CF. UVA-induced cell cycle progression is mediated by a disintegrin and metalloprotease/epidermal growth factor receptor/AKT/cyclin D1 pathways in keratinocytes. *Cancer Res*. 2008;68(10):3752. doi:10.1158/0008-5472.CAN-07-6138
30. Ma H, Brennan A, Diamond SA. Phototoxicity of TiO_2 nanoparticles under solar radiation to two aquatic species: daphnia magna and Japanese medaka. *Environ Toxicol Chem*. 2012;31(7):1621–1629. doi:10.1002/etc.v31.7
31. Xue C, Luo W, Yang X. A mechanism for nano-titanium dioxide-induced cytotoxicity in HaCaT cells under UVA irradiation. *Biosci Biotechnol Biochem*. 2015;79(8):1384–1390. doi:10.1080/09168451.2015.1023248

32. Fu L, Hamzeh M, Dodard S, Zhao YH, Sunahara GI. Effects of TiO_2 nanoparticles on ROS production and growth inhibition using freshwater green algae pre-exposed to UV irradiation. *Environ Toxicol Pharmacol*. 2015;39(3):1074–1080. doi:10.1016/j.etap.2015.03.015
33. Wu Y, Geis-Gerstorfer J, Scheideler L, Rupp F. Photocatalytic antibacterial effects on TiO_2-anatase upon UV-A and UV-A/VIS threshold irradiation. *Biofouling*. 2016;32(5):583–595. doi:10.1080/08927014.2016.1170118
34. Patist CM, Mulder MB, Gautier SE, Maquet V, Jérôme R, Oudega M. Freeze-dried poly(d,l-lactic acid) macroporous guidance scaffolds impregnated with brain-derived neurotrophic factor in the transected adult rat thoracic spinal cord. *Biomaterials*. 2004;25(9):1569–1582. doi:10.1016/S0142-9612(03)00503-9
35. Taylor SJ, Rosenzweig ES, McDonald JW, Sakiyama-Elbert SE. Delivery of neurotrophin-3 from fibrin enhances neuronal fiber sprouting after spinal cord injury. *J Controlled Release*. 2006;113(3):226–235. doi:10.1016/j.jconrel.2006.05.005
36. Mahmoudi M, Azadmanesh K, Shokrgozar MA, Journeay WS, Laurent S. Effect of nanoparticles on the cell life cycle. *Chem Rev*. 2011;111(5):3407–3432. doi:10.1021/cr1003166
37. Burdette JE, Jeruss JS, Kurley SJ, Lee EJ, Woodruff TK. Activin a mediates growth inhibition and cell cycle arrest through smads in human breast cancer cells. *Cancer Res*. 2005;65(17):7968. doi:10.1158/0008-5472.CAN-04-3553
38. Ko J-W, Shin N-R, Park J-W, et al. Copper oxide nanoparticles induce collagen deposition via TGF-β1/Smad3 signaling in human airway epithelial cells. *Nanotoxicology*. 2018;12(3):239–250. doi:10.1080/17435390.2018.1432778
39. Senturk S, Mumcuoglu M, Gursoy-Yuzugullu O, Cingoz B, Akcali KC, Ozturk M. Transforming growth factor-beta induces senescence in hepatocellular carcinoma cells and inhibits tumor growth. *Hepatology*. 2010;52(3):966–974. doi:10.1002/hep.23769
40. Hong-Sheng C, Ming-Han B, Tao Z, Guo-Dong L, Ming L. Ellagic acid induces cell cycle arrest and apoptosis through TGF-β/Smad3 signaling pathway in human breast cancer MCF-7 cells. *Int J Oncol*. 2015;46(4):1730–1738. doi:10.3892/ijo.2015.2870
41. Puente Bao N, Kimura W, Muralidhar Shalini A, et al. The oxygen-rich postnatal environment induces cardiomyocyte cell-cycle arrest through DNA damage response. *Cell*. 2014;157(3):565–579. doi:10.1016/j.cell.2014.03.032
42. Eva C-M, Esther B, Isabel F. Cross-talk between TGF-β and NADPH oxidases during liver fibrosis and hepatocarcinogenesis. *Curr Pharm Des*. 2015;21(41):5964–5976. doi:10.2174/1381612821666151029112126
43. Sun S, Xie F, Zhang Q, et al. Advanced oxidation protein products induce hepatocyte epithelial–mesenchymal transition via a ROS-dependent, TGF-β/Smad signaling pathway. *Cell Biol Int*. 2017;41(8):842–853. doi:10.1002/cbin.v41.8